Dynamic two-dimensional refractive index modulation for high performance acousto-optic deflector

Tiansi Wang,[1] Chong Zhang,[2] Aleksandar Aleksov,[3] Islam A. Salama,[2] and Aravinda Kar[1]

[1]*CREOL, The College of Optics & Photonics Mechanical and Aeronautical Engineering and Material Science Engineering Department University of Central Florida, P.O. Box 162700, Orlando, FL 32816-2700, USA*
[2]*Intel - Assembly & Test Technology Development 5000 W Chandler Blvd, Chandler, AZ 85226 USA*
[3]*Intel – Components research 5000 W Chandler Blvd, Chandler, AZ 85226 USA*
[*]*akar@creol.ucf.edu*

Abstract: The performance of an acousto-optic deflector is studied for two-dimensional refractive index that varies as periodic and sinc functions in the transverse and longitudinal directions, respectively, with respect to the direction of light propagation. Phased array piezoelectric transducers can be operated at different phase shifts to produce a two-dimensionally inhomogeneous domain of phase grating in the acousto-optic media. Also this domain can be steered at different angles by selecting the phase shift appropriately. This mechanism of dynamically tilting the refractive index-modulated domain enables adjusting the incident angle of light on the phase grating plane without moving the light source. So the Bragg angle of incidence can be always achieved at any acoustic frequency, and consequently, the deflector can operate under the Bragg diffraction condition at the optimum diffraction efficiency. Analytic solutions are obtained for the Bragg diffraction of plane waves based on the second order coupled mode theory, and the diffraction efficiency is found to be unity for optimal index modulations at certain acoustic parameters.

OCIS codes: (230.1950) Diffraction gratings; (230.1040) Acousto-optical devices.

References and links

1. G. D. Reddy, R. J. Cotton, A. S. Tolias, and P. Saggau, "Random-access multiphoton microscopy for fast three-dimensional imaging," in *Membrane Potential Imaging in the Nervous System and Heart*, M. Canepari, D. Zecevic, and O. Bernus, ed. (Springer, 2015), Ch. 18.
2. J.-C. Kastelik, S. Dupont, K. B. Yushkov, and J. Gazalet, "Frequency and angular bandwidth of acousto-optic deflectors with ultrasonic walk-off," Ultrasonics **53**(1), 219–224 (2013).
3. W. R. Klein and B. D. Cook, "Unified approach to ultrasonic light diffraction," IEEE Trans. Sonics Ultrason. **14**(3), 123–134 (1967).
4. R. S. Chu and T. Tamir, "Guided-wave theory of light diffraction by acoustic microwaves," IEEE Trans. Microw. Theory Tech. **18**(8), 486–504 (1970).
5. H. Kogelnik, "Coupled wave theory for thick hologram gratings," Bell Syst. Tech. J. **48**(9), 2909–2947 (1969).
6. F. G. Kaspar, "Diffraction by thick, periodically stratified gratings with complex dielectric constant," J. Opt. Soc. Am. A **63**(1), 37–45 (1973).
7. C. B. Burckhardt, "Diffraction of a plane wave at a sinusoidally stratified dielectric grating," J. Opt. Soc. Am. **56**(11), 1502–1508 (1966).
8. T. K. Gaylord and M. G. Moharam, "Planar dielectric grating diffraction theories," Appl. Phys. B **28**(1), 1–14 (1982).
9. R. S. Chu and T. Tamir, "Bragg diffraction of Gaussian beams by periodically modulated media," J. Opt. Soc. Am. **66**(3), 220–226 (1976).
10. R. S. Chu and T. Tamir, "Diffraction of Gaussian beams by periodically modulated media for incidence close to a Bragg angle," J. Opt. Soc. Am. **66**(12), 1438–1440 (1976).
11. R. S. Chu, J. A. Kong, and T. Tamir, "Diffraction of Gaussian beams by a periodically modulated layer," J. Opt. Soc. Am. **67**(11), 1555–1561 (1977).
12. M. G. Moharam, T. K. Gaylord, and R. Magnusson, "Bragg diffraction of finite beams by thick gratings," J. Opt. Soc. Am. **70**(3), 300–304 (1980).

#253296 Received 5 Nov 2015; revised 3 Dec 2015; accepted 7 Dec 2015; published 21 Dec 2015

13. N. Uchida and N. Niizeki, "Acoustooptic deflection materials and techniques," Proc. IEEE **61**(8), 1073–1092 (1973).
14. J. A. Kong, "Second-order coupled-mode equations for spatially periodic media," J. Opt. Soc. Am. **67**(6), 825–829 (1977).
15. J.-M. Andre, K. L. Guen, and P. Jonnard, "Rigorous coupled-wave theory for lossy volume grating in Laue geometry X-ray spectroscopy," hal-01082017 (2014).
16. L. Azar, Y. Shi, and S.-C. Wooh, "Beam focusing behavior of linear phased arrays," NDT Int. **33**(3), 189–198 (2000).
17. X. Zhao and T. Gang, "Nonparaxial multi-Gaussian beam models and measurement models for phased array transducers," Ultrasonics **49**(1), 126–130 (2009).
18. K. Nakahata and N. Kono, "3-D modelings of an ultrasonic phased array transducer and its radiation properties in solid," in *Ultrasonic Waves*, A. A. dos Santos, Jr., ed. (InTech, 2012), p. 59–80.
19. M. Gottlieb, L. M. Ireland, and J. M. Ley, *Electro-Optic and Acousto-Optic Scanning and Deflection* (Marcel Dekker, 1983).
20. S.-C. Wooh and Y. Shi, "Influence of phased array element size on beam steering behavior," Ultrasonics **36**(6), 737–749 (1998).
21. S.-C. Wooh and Y. Shi, "Optimum beam steering of linear phased arrays," Wave Motion **29**(3), 245–265 (1999).
22. S.-C. Wooh and Y. Shi, "A simulation Study of the beam steering characteristics for linear phased arrays," JNE **18**, 39–57 (1999).
23. A. Korpel, *Acousto-Optics* (CRC Press, 1997).
24. B. M. Watrasiewicz, "Some useful integrals of Si(x), Ci(x) and related integrals," Opt. Acta (Lond.) **14**(3), 317–322 (1967).
25. F. G. Tricomi, *Integral Equations* (Dover, 1985).
26. J. A. Kong, *Electromagnetic Wave Theory*, 2nd ed. (Wiley, 1990).
27. J. P. Xu and R. Stroud, *Acousto-Optic Devices: Principles, Design, and Applications* (Wiley, 1982).
28. N. Uchida and Y. Ohmachi, "Elastic and photoelastic properties of TeO_2 single crystal," J. Appl. Phys. **40**(12), 4692–4695 (1969).
29. A. P. Goutzoulis and V. V. Kludzin, Principles of acousto-optics" in *Design and Fabrication of Acousto-Optic Devices*, A. P. Goutzoulis and D. R. Pape, ed. (Marcel Dekker, 1994).
30. D. R. Pape, O. B. Gusev, S. V. Kulakov, and V. V. Momotok, "Design of acousto-optic deflectors" in *Design and Fabrication of Acousto-Optic Devices*, A. P. Goutzoulis and D. R. Pape, eds. (Marcel Dekker, 1994).

1. Introduction

The light diffraction by bulk acoustic waves is a subject of considerable interest due to the wide variety of important applications. Bulkwave acousto-optics enable spatial, temporal and spectral modulations of light in various devices such as acousto-optic deflectors (AODs), acousto-optic modulators and acousto-optic tunable filters. Specifically, in medical applications, AODs enable inertia-free scanning for fast two-dimensional and three-dimensional imaging in multiphoton microscopy on physiologically relevant time scales, overcoming the limitations of galvanometer scanners [1]. Therefore, the diffraction characteristics of acousto-optic gratings have been analyzed extensively. These studies can be broadly distinguished depending on the sizes of the incident light and acousto-optic medium. The light can be plane waves of infinite dimension laterally or a beam of finite size, and similarly, the medium can be the half-space or a crystal of finite length. Additionally, the medium can be isotropic or anisotropic. Kastelik et al. [2] analyzed the performance of anisotropic acousto-optic crystals by introducing a phase mismatch vector in the method of wave vector diagram.

Klein and Cook [3] studied the diffraction of light due to ultrasonic waves by solving a set of coupled first order difference-differential equations that were obtained from the optical wave equation by applying the method of partial wave, which involves resolving the diffracted light into a series of plane waves, and neglecting the second order derivatives of the amplitude of the electric field. Chu and Tamir [4] presented a rigorous modal approach as well as a coupled mode representation for the diffraction of light in periodically modulated isotropic media. Although the modal theory is accurate, it is tedious and time-consuming for determining the solution. Kogelnik [5] developed a coupled wave approach, which yields analytic results that are accurate around the Bragg angle of incidence for the Klein-Cook parameter greater than 10. Kaspar [6] applied Burckhardt's [7] Floquet method to thick gratings and compared the results to the coupled wave model. Burckhardt's work was only for phase gratings, which was extended to phase-plus-absorption gratings by Kaspar. Gaylord and Moharam [8] analyzed the coupled wave theory and showed the similarity between the

#253296 Received 5 Nov 2015; revised 3 Dec 2015; accepted 7 Dec 2015; published 21 Dec 2015

coupled wave and modal approaches. These studies were for the diffraction of plane waves rather than the practical case of light beams of finite size. However, Chu and Tamir [9,10], and Chu, Kong and Tamir [11] applied the coupled mode theory to Gaussian beams by considering the beam as a superposition of plane waves. Moharam, Gaylord and Magnusson [12] studied the diffraction of Gaussian beams in acousto-optic media using a modified version of the coupled wave theory, yielding two coupled first order partial differential equations.

Chu and Tamir [3,9,10] simplified the coupled mode equations under the assumption of slowly-varying electric field, $E(x)$, such that $\left|d^2E(x)/dx^2\right| \ll \left|k_{0x}dE(x)/dx\right|$ where k_x is the angular wavevector in the direction, *x*, of the light propagation. This approximation, which is generally applicable to weakly-modulated media, yielded two coupled first order ordinary differential equations. They solved the equations analytically by neglecting the reflection of energy at the exit boundary and, therefore, the solution is applicable to the propagation of light in very wide media and the half-space. Uchida and Niizeki [13] studied a first order coupled mode theory that yielded analytic solutions for 0 and −1 order modes at the Bragg angle of incidence. However, the application of their model is restricted to weakly modulated media [11] since it neglects the effect of the exit boundary. Later Kong [14] presented a simplified second order coupled mode approach for both weakly and strongly modulated media and provided analytic solutions for the reflection and transmission coefficients, accounting for the effects at both boundaries of an AOD.

The above-mentioned studies are, however, based on one-dimensional modulation of the refractive index. Only recently, attention has been paid to the effect of two-dimensional refractive index modulation on light diffraction as analyzed by Andre, Guen and Jonnard [15]. In the present paper, the diffraction of plane wave lights is studied in two-dimensionally modulated media of finite size. The bulk acousto-optic grating is formed by the interaction of light and acoustic waves. The acoustic wave is steerable [16–18] using a phased array of transducers with suitable time delayed radio-frequency (RF) signals. This mechanism enables meeting the Bragg condition at every RF frequency for incident lights from a fixed source. Consequently, the dynamic acousto-optic volume grating can improve the performance of AODs, such as high diffraction efficiency, large deflection angle and large scan angle.

This paper begins by presenting in Section 2 a qualitative argument that supports the coupled-mode theory of light diffraction based on two-dimensional refractive index modulation. An analytic approach is then presented for second-order coupled mode propagation of light in AODs with multiple phased-array transducers. The results are presented in Section 3 for TeO_2 AODs based on the phase, frequency and amplitude modulations of the transducers. Additionally, the diffraction efficiency of this two-dimensional refractive index model is compared to the results of others' one-dimensional refractive index models.

2. Theoretical background

2.1 Modulation of refractive index in two dimensions

Conventional AODs are operated with a single transducer or an array of transducers assembled in the planar or stepped configuration [19]. In the single transducer configuration, the performance of AODs is limited by the applied RF power, narrow bandwidth, small deflection angle, narrow scan angle and low diffraction efficiency.

#253296 Received 5 Nov 2015; revised 3 Dec 2015; accepted 7 Dec 2015; published 21 Dec 2015

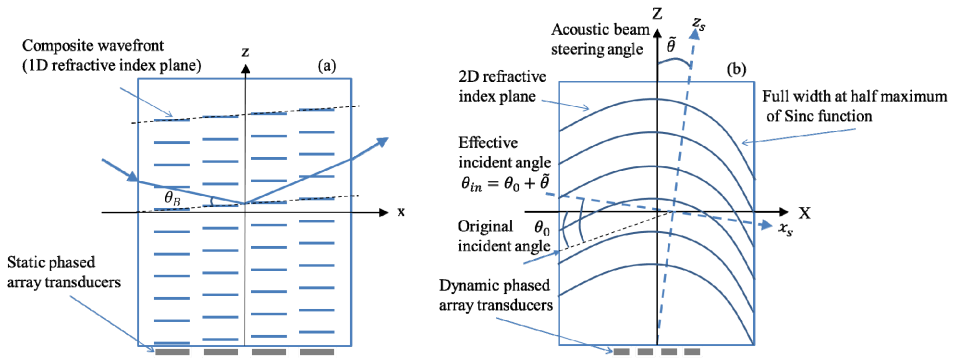

Fig. 1. Difference in the refractive index profiles due to Fig. 1(a) static phased array transducers in conventional AOD and Fig. 1(b) dynamic phased array transducers in this study.

The array configuration of transducers was introduced to improve the performance of AODs using phase-shifted acoustic waves that create tilted modulation in the refractive index as shown in Fig. 1(a). Each transducer is operated at a relative time delay to generate phase-shifted acoustic waves. These waves propagate through the AOD with a tilted composite wavefront and consequently, the compressed and rarefied atomic layers are also tilted resulting in the slanted refractive index modulation. This type of transducer array improves the deflection scan angle and the diffraction efficiency. However, the time delays are fixed, which produce a static phase grating, and the transducers are relatively large in conventional AODs and therefore, the composite wavefronts cannot be steered at any arbitrary angles. Dynamic phase gratings can be produced by operating the transducers at different phase shifts and utilizing the interference and diffraction of the acoustic waves. These phenomena produce a tilted grating lobe with the principal direction, z_s, as shown in Fig. 1(b) and the lobe can be steered at any angle of interest by varying the phase shift and amplitude of the acoustic waves.

The steering angle is indicated by $\tilde{\theta}$ in Fig. 1(b). Noting that θ_0 is the original incident angle of the light onto the unperturbed medium, the new incident angle becomes $\theta_{in} = \theta_0 + \tilde{\theta}$ for the tilted lobe. Thus the tilted lobe provides a mechanism of automatically changing the incident angle of light without moving the original light source. Also the frequency of the acoustic waves emitted by the transducers can be adjusted to achieve the Bragg angle of incidence, i.e., $\theta_{in} = \theta_B$ for each lobe, which ensures large deflection angle given by θ_{in} and large diffraction efficiency given by the Bragg diffraction condition.

Another aspect of the tilted lobe is two-dimensional modulation of refractive index in the lobe, which results in dynamic two-dimensional gratings in contrast to one-dimensional gratings in conventional AODs. The interference and diffraction of the acoustic waves that form the lobe, also produce a resultant acoustic intensity distribution as a diffraction pattern, typically, in the form of a sinc function. This intensity pattern modifies the refractive index in the transverse direction x_s, and the index variation is taken as a sinc function in this study. On the other hand, the refractive index varies periodically with the period Λ in the longitudinal direction z_s due to the propagation of the acoustic waves in the AOD. These two mechanisms produce a refractive index profile in two dimensions by perturbing the nominal refractive index in the titled lobe as shown in Fig. 2, resulting in a two-dimensional phase grating. Wooh and Shi [20–22] showed that multiple piezoelectric transducers can produce steerable acoustic lobes in a medium, and the longitudinal direction, z_s, coincides with the composite acoustic wavevector $\vec{K}$. A typical two-dimensional index profile in region II, $n_{II}(x,z)$, can be written as:

#253296 Received 5 Nov 2015; revised 3 Dec 2015; accepted 7 Dec 2015; published 21 Dec 2015

$$n_{II}(x,z) = n_2(\lambda_0) + \Delta n \cos\left(\frac{2\pi}{\Lambda} z\right)\left(\frac{\sin(bx)}{bx}\right) \tag{1}$$

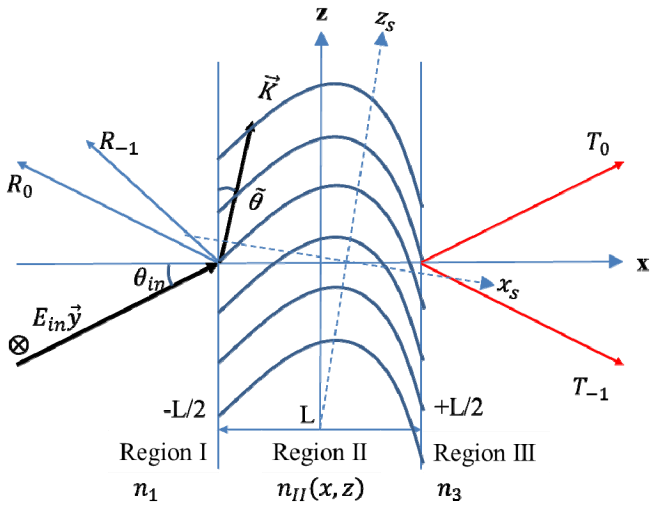

Fig. 2. Two-dimensional refractive index profile generated by a tilted lobe in an acousto-optic medium.

where $n_2(\lambda_0)$ is the refractive index of the unperturbed acousto-optic medium at the wavelength of the incident light in vacuum, λ_0, and Δn and Λ are the maximum change in the refractive index and the acoustic wavelength in the modulated medium, respectively. The parameter b is a constant that defines the length of the lobe spanned by the central peak of the sinc function with significant contribution to Δn. Considering that x = 0 is at the center of the lobe, x = ± L/2 represent two points on either side of the center, and L is the full width at half maximum of the sinc function, b can be related to L by the following expression:

$$\frac{\sin(bL/2)}{bL/2} = 1/2 \tag{2}$$

The perturbation of the refractive index, δn, from its nominal value, $n_2(\lambda_0)$, is given by [21]:

$$\delta n = -\frac{1}{2} n_2^3(\lambda_0)\, pe \tag{3}$$

where p is the photo-elastic constant and e is the strain tensor due to the mechanical stresses induced by the acoustic wave. The strain amplitude is in the range of 10^{-8} to 10^{-5}, and the photoelastic coefficient is 0.23 for TeO_2 [19]. So the value of δn and consequently, the maximum modulation, Δn, are relatively small for typical AODs.

2.2 Second order coupled-mode equations for periodically modulated media

For an incident light of TE polarization in the y direction, the electric field, $E_{II}(x,z)$, satisfies the following scalar wave equation in the modulated region II bounded by $-L/2 \le x \le L/2$,

$$\left[\frac{\partial^2}{\partial x^2} + \frac{\partial^2}{\partial z^2} + k_0^2 n_{II}^2(x,z)\right] E_{II,y}(x,z) = 0 \tag{4}$$

#253296 Received 5 Nov 2015; revised 3 Dec 2015; accepted 7 Dec 2015; published 21 Dec 2015

where k_0 is the angular wavenumber of the light at its wavelength in vacuum. Since the light propagates in a periodic medium of periodicity Λ, and the wavevector of the acoustic field, $\vec{K}$, is inclined to the z axis at an angle $\tilde{\theta}$ (Fig. 2), the electric field can be expanded in a set of Floquet waves [14],

$$E_{II,y}(x,z) = \sum_{m=-\infty}^{\infty} E_m(x) e^{im\pi/2} e^{i\kappa_{mz} z} \tag{5}$$

where

$$\kappa_{mz} = k_{0z} + mK\cos\tilde{\theta} \tag{6}$$

E_m is the m-th mode electric field, k_{0z} is the z component of the wavevector of the light inside Region II at the incident boundary, and K is the angular wavenumber of the acoustic wave in this region, i.e., $K = 2\pi/\Lambda$. Applying Eq. (4) to Eq. (3) and equating the coefficient of the m-th Floquet wave to zero, the following second order coupled mode equation is obtained.

$$\frac{d^2E_m(x)}{dx^2} + \left(k_2^2 - \kappa_{mz}^2\right)E_m(x) + i\frac{\Delta n}{n_2}\left(\frac{\sin(bx)}{bx}\right)k_2^2\left(E_{m+1} - E_{m-1}\right) = 0 \tag{7}$$

At the Bragg angle of incidence and in its vicinity, only two Floquet modes, i.e., $E_0(x)$ and $E_{-1}(x)$ modes, couple strongly to each other. So Eq. (7) can be reduced to the following two coupled equations by neglecting the higher order modes and taking $\tilde{\theta}$ as zero.

$$\frac{d^2E_0}{dx^2} + \frac{\phi_1^2}{L^2}E_0 = i\frac{\phi\phi_1}{L^2}\left(\frac{\sin(bx)}{bx}\right)E_{-1} \tag{8}$$

$$\frac{d^2E_{-1}}{dx^2} + \frac{\phi_1^2\beta^2}{L^2}E_{-1} = -i\frac{\phi\phi_1}{L^2}\left(\frac{\sin(bx)}{bx}\right)E_0 \tag{9}$$

Three dimensionless parameters, ϕ_1, ϕ and β, appear in Eqs. (8) and (9), which are given by:

$$\phi_1 = k_0 n_2 L\cos\theta_2 \tag{10}$$

$$\phi = \frac{k_0\Delta nL}{\cos\theta_2} \tag{11}$$

$$\beta = \sqrt{1 - \frac{Q}{\phi_1}(1-\alpha)} \tag{12}$$

where Q and α are Klein-Cook parameter and angle ratio, respectively, which are defined below. The relations $k_{0z} = k_2\sin\theta_2$ and $k_2 = n_2k_0$ are used to obtain ϕ_1 while deriving Eqs. (8) and (9), where θ_2 is the angle of refraction at the incident boundary of the AOD medium. ϕ_1 is a phase parameter for the light in the unperturbed medium.

ϕ, which is obtained using the relation $k_2 = n_2k_0$ while deriving Eqs. (8) and (9), represents the phase difference due to the change in the optical path length ΔnL. This

#253296 Received 5 Nov 2015; revised 3 Dec 2015; accepted 7 Dec 2015; published 21 Dec 2015

parameter can be varied by operating the piezoelectric transducer in the amplitude modulation mode since Δn depends on the amplitude of the acoustic wave. The third parameter β includes the light-sound interactions through the Klein-Cook parameter Q and the angle ratio α. The relations $k_{0z} = k_2 \sin\theta_2$ and $k_2 = n_2 k_0$ are used to obtain β while deriving Eqs. (8) and (9).

Q is given by [23]:

$$Q = \frac{K^2 L}{n_2 k_0 \cos\theta_2} \tag{13}$$

It classifies the light diffraction process into three regimes: (i) Raman-Nath diffraction in thin gratings corresponding to $Q \ll 1$, (ii) Bragg diffraction in thick gratings corresponding to $Q \gg 1$, and (iii) the transition region for $Q \approx 1$. The angle ratio, α, is defined as:

$$\alpha = \frac{2k_0 \sin\theta_{in}}{K} \tag{14}$$

It represents the ratio of the sine functions of the incident and Bragg angles since $\sin\theta_B = K/(2k_0)$, where θ_B is the Bragg angle measured outside the acousto-optic medium. The sine of an angle is approximately equal to the angle itself for small angles, and under this condition, α is a measure of the incident angle normalized by the Bragg angle. α = 1 indicates $\theta_{in} = \theta_B$ and $\alpha > 1$ corresponds to $\theta_{in} > \theta_B$. The angle ratio parameter can be varied by operating the piezoelectric transducers in the frequency modulation mode since K depends on the frequency of the acoustic wave.

2.3 Solutions of the reduced coupled mode equations

Equations (8) and (9) are solved for 0 and −1 order Floquet modes $E_0(x)$ and $E_{-1}(x)$, respectively, by the method of variation of parameters. The resulting expressions, which involve the sine integral, $Si(z)$, and cosine integral, $Ci(z)$ [24], are given below:

$$\begin{aligned}
E_0(x) &= A_1 e^{i\frac{\phi_1}{L}x} + A_2 e^{-i\frac{\phi_1}{L}x} \\
&+ \frac{i\phi}{4bL} B_1 \sum_{j=1}^{4} \left[1 - 2\delta_{j1} - 2\delta_{j2}\right] e^{i(-1)^{j-1}\frac{\phi_1}{L}x} \left[Si(b_{1j}x) - iCi(b_{1j}x)\right] \\
&+ \frac{i\phi}{4bL} B_2 \sum_{j=1}^{4} \left[1 - 2\delta_{j1} - 2\delta_{j2}\right] e^{i(-1)^{j-1}\frac{\phi_1}{L}x} \left[Si(b_{2j}x) - iCi(b_{2j}x)\right] \\
&+ \frac{\phi^2}{4\beta L^2} \sum_{j=1}^{2} (-1)^j e^{i(-1)^{j-1}\frac{\phi_1}{L}x} \int_0^x e^{i(-1)^{2-j}\frac{\phi_1}{L}x''} \frac{\sin(bx'')}{bx''} \\
&\times \left[\sum_{p=1}^{2} (-1)^p e^{i(-1)^{p-1}\frac{\phi_1\beta}{L}x''} \int_0^{x''} e^{i(-1)^{2-p}\frac{\phi_1\beta}{L}x'} \frac{\sin(bx')}{bx'} E_0(x')dx'\right] dx''
\end{aligned} \tag{15}$$

#253296 Received 5 Nov 2015; revised 3 Dec 2015; accepted 7 Dec 2015; published 21 Dec 2015

$$
\begin{aligned}
E_{-1}(x) &= B_1 e^{i\frac{\phi_1\beta}{L}x} + B_2 e^{-i\frac{\phi_1\beta}{L}x} \\
&+ \frac{i\phi}{4bL\beta} A_1 \sum_{j=1}^{4} \left[1 - 2\delta_{j1} - 2\delta_{j2}\right] e^{i(-1)^{j-1}\frac{\phi_1\beta}{L}x} \left[Si\left(a_{1j}x\right) - iCi\left(a_{1j}x\right)\right] \\
&+ \frac{i\phi}{4bL\beta} A_2 \sum_{j=1}^{4} \left[1 - 2\delta_{j1} - 2\delta_{j2}\right] e^{i(-1)^{j-1}\frac{\phi_1\beta}{L}x} \left[Si\left(a_{2j}x\right) - iCi\left(a_{2j}x\right)\right] \\
&+ \frac{\phi^2}{4\beta L^2} \sum_{j=1}^{2} (-1)^j e^{i(-1)^{j-1}\frac{\phi_1\beta}{L}x} \int_0^x e^{i(-1)^{2-j}\frac{\phi_1\beta}{L}x''} \frac{\sin(bx'')}{bx''} \\
&\times \left[\sum_{p=1}^{2} (-1)^p e^{i(-1)^{p-1}\frac{\phi_1}{L}x''} \int_0^{x''} e^{i(-1)^{2-p}\frac{\phi_1}{L}x'} \frac{\sin(bx')}{bx'} E_{-1}(x')dx'\right] dx''
\end{aligned}
\tag{16}
$$

where δ_{j1} and δ_{j2} are Kronecker's delta functions and the other auxiliary parameters are defined as:

$$
\begin{aligned}
b_{11} = a_{24} &= b - \frac{\phi_1}{L}(1-\beta), b_{21} = a_{21} = b - \frac{\phi_1}{L}(1+\beta) \\
b_{12} = a_{12} &= -b + \frac{\phi_1}{L}(1+\beta), b_{22} = a_{13} = -b + \frac{\phi_1}{L}(1-\beta) \\
b_{13} = a_{22} &= -b - \frac{\phi_1}{L}(1-\beta), b_{23} = a_{23} = -b - \frac{\phi_1}{L}(1+\beta) \\
b_{14} = a_{14} &= b + \frac{\phi_1}{L}(1+\beta), b_{24} = a_{11} = b + \frac{\phi_1}{L}(1-\beta)
\end{aligned}
\tag{17}
$$

A_1, A_2, and B_1 and B_2 are the constants pertaining to the homogeneous solutions for 0 and −1 order Floquet modes, $E_0(x)$ and $E_{-1}(x)$, respectively. On the right hand side in Eqs. (16) and (17), the first two terms are these two modes in the unperturbed acousto-optic medium and the third and fourth terms represent the interaction between these two modes in the perturbed medium for transferring energy between them. The last term in each equation represents higher order effects for the interaction between the modes involving $(\Delta n)^2$ through the ϕ^2 term. This last term also shows the self-effect of each mode because the electric field of a mode at a given point x, e.g., $E_0(x)$, is affected by the distribution of the field over the entire distance ranging from 0 to x. Equations (16) and (17) are essentially Volterra integral equations which can be solved by the method of successive approximations [25]. As a first approximation, however, only the first four terms have been considered in this study to calculate $E_0(x)$ and $E_{-1}(x)$.

2.4 Reflection and transmission due to the modulated medium

In region I, the overall electric field, which consists of the incident and reflected fields, can be expressed as:

$$
E_{I,y}(x,z) = G_m e^{ik_{in,mx}x} e^{ik_{in,mz}z} + r_0 e^{-i\kappa_{1,0x}x} e^{i\kappa_{0z}z} + r_{-1} e^{-i\kappa_{1,-1x}x} e^{i\kappa_{-1z}z} \tag{18}
$$

where G_m is the amplitude of m-th plane wave component of the input light, $k_{in,mx}$ is the x component of the wavevector of the incident m-th plane wave component, r_0 and r_{-1} are the field reflection coefficients for 0 and −1 Floquet modes, respectively, and $\kappa_{1,0x}$ and $\kappa_{1,-1x}$ are the x components of the wavevectors for 0 and −1 Floquet modes, respectively, in region I, as

#253296 Received 5 Nov 2015; revised 3 Dec 2015; accepted 7 Dec 2015; published 21 Dec 2015

given later in this section. κ_{0z} and κ_{-1z} are the z components of the wavevectors for 0 and −1 Floquet modes, respectively.

In region II, the electric field takes the form:

$$E_{II,y}(x,z) = E_0(x)e^{i\kappa_{0z}z} - iE_{-1}(x)e^{i\kappa_{-1z}z} \tag{19}$$

where $E_0(x)$ and $E_{-1}(x)$ are the solutions to the two Floquet modes given by Eqs. (15) and (16), respectively.

In region III, the electric field consists of the transmitted components of 0 and −1 order modes, and there is no reflection from this region back to region II. So the transmitted electric field in region III can be written as:

$$E_{III,y}(x,z) = t_0 e^{i\kappa_{3,0x}x} e^{i\kappa_{0z}z} + t_{-1} e^{i\kappa_{3,-1x}x} e^{i\kappa_{-1z}z} \tag{20}$$

where t_0 and t_{-1} are the field transmission coefficients for 0 and −1 Floquet modes, respectively, and $\kappa_{3,0x}$ and $\kappa_{3,-1x}$ are the x components of the wave vectors for 0 and −1 Floquet modes, respectively, as given below.

The $\hat{x}$ components of the wave vectors pertaining to the Floquet modes are given by:

$$\kappa_{r,mx} = \sqrt{k_r^2 - \kappa_{mz}^2} \tag{21}$$

where $\kappa_{r,mx}$ is the x component of the wavevector in region r, r = 1 or 3, respectively, for m-th Floquet mode. Equations (18)-(20) contain eight unknowns: r_0, r_{-1}, A_1, A_2, B_1, B_2, t_0 and t_{-1}, which are determined by applying the boundary conditions that the tangential electric and magnetic fields are continuous at the incident (x = -L/2) and exit (x = L/2) boundaries of the acousto-optic medium. The boundary conditions involving the normal components, which require that the normal component of the electric displacement vector and the normal component of the magnetic flux density vector be continuous at the boundaries, are not considered because these two conditions are not independent of the two tangential conditions [26]. Since the tangential magnetic field H_z is given by Maxwell's equation as $H_z = \frac{1}{i\omega\mu}\frac{\partial E_y}{\partial x}$, where μ is the permeability of a given medium, the boundary conditions can be written as follows for nonmagnetic media, i.e., $\mu = 1$.

$$\text{At } x = -L/2,\ E_{I,y}(x,z) = E_{II,y}(x,z) \text{ and } \frac{\partial E_{I,y}}{\partial x} = \frac{\partial E_{II,y}}{\partial x} \tag{22}$$

$$\text{At } x = L/2,\ E_{II,y}(x,z) = E_{III,y}(x,z) \text{ and } \frac{\partial E_{II,y}}{\partial x} = \frac{\partial E_{III,y}}{\partial x} \tag{23}$$

These four boundary conditions must be satisfied for each mode at all values of z. So eight linear simultaneous equations can be obtained by equating the coefficients of the waveform of each mode, i.e., $e^{i\kappa_{0z}z}$ or $e^{i\kappa_{-1z}z}$, to zero for determining the eight unknowns. The Crammer rule is applied in this study to calculate these unknown coefficients.

The solution is verified by checking that the Conservation of Energy (CoE) is satisfied. The transmitted and diffracted electric fields, E_0 and E_{-1}, respectively, are related to the electric field of the incident light, E_{in}, by the CoE as stated below:

$$\left(\frac{\kappa_{1,0x}}{k_{1x}}\right)|r_0|^2 + \left(\frac{\kappa_{1,-1x}}{k_{1x}}\right)|r_{-1}|^2 + \left(\frac{\kappa_{3,0x}}{k_{1x}}\right)|t_0|^2 + \left(\frac{\kappa_{3,-1x}}{k_{1x}}\right)|t_{-1}|^2 = 1 \tag{24}$$

#253296 Received 5 Nov 2015; revised 3 Dec 2015; accepted 7 Dec 2015; published 21 Dec 2015

for the case of $G_m = 1.0$.

3. Results and discussion

In this study, the acousto-optic medium is a TeO_2 crystal, which is transparent in the wavelength range of 0.35 to 5 μm [13,27], and the incident light is a plane wave of wavelength $\lambda_0 = 632.8$ nm in vacuum. So the angular wavenumber of the light in vacuum is $k_0 = 9.93 \times 10^6$ m^{-1}. The nominal refractive index of the crystal is $n_2 = 2.26$ at this wavelength, which is the refractive index for the ordinary light [28]. Although TeO_2 is a uniaxial positive crystal, it can be treated as an isotropic medium for longitudinal acoustic waves and transverse electric polarized light. The velocity of sound in the crystal is V = 4260 m/s in the crystallographic direction [001] for the longitudinal mode [28] that results in $\Lambda = 56$ μm and $K = 1.12 \times 10^5$ m^{-1}. So the Bragg angle of incidence is $\theta_B = 0.324°$ at 75 MHz. The length of the modulated region is L = 2.24 cm, which yields $Q = 4\pi$ and therefore, the AOD is operated in the Bragg regime since Q >> 1.

Results are obtained for different cases by varying the frequency of the acoustic waves as well as their amplitudes and phases. The effect of amplitude modulation manifests as the index modulation Δn, and the phase-shifting corresponds to grating lobes at different steering angles, $\tilde{\theta}$, resulting in a new incident angle $\theta_0 + \tilde{\theta}$ [Fig. 1(b)]. This angle would be the Bragg angle of incidence if the acoustic frequency for the lobe is chosen properly using the Bragg diffraction condition, i.e., $\sin\left(\theta_0 + \tilde{\theta}\right) = \lambda_0 F / (2V)$. Thus the effect of phase-shifting manifests as operating the AOD under the Bragg diffraction condition for each lobe to achieve large deflection angle, $\theta_0 + \tilde{\theta}$, and high diffraction efficiency at any frequency. Four parameters, the index modulation strength Δn, the acoustic frequency F, the angle of incidence θ_{in} and the grating length L, are found to affect the optimal performance of the AOD.

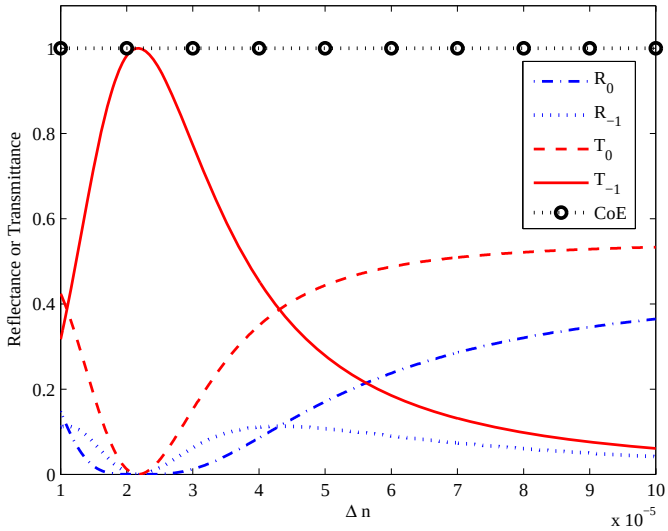

Fig. 3. Reflectance and Transmittance as a function of the index modulation strength Δn with L = 2.24 cm, Q = 4π and F = 75 MHz at Bragg incidence angle of 0.324°.

The solutions of the above-mentioned eight linear algebraic equations yield the reflection and transmission coefficients, r_0, r_{-1}, t_0 and t_{-1}, for 0 and −1 order modes. The corresponding reflectance and transmittance are given by $R_0 = |r_0|^2, R_{-1} = |r_{-1}|^2$ and $T_0 = |t_0|^2, T_{-1} = |t_{-1}|^2$,

#253296 Received 5 Nov 2015; revised 3 Dec 2015; accepted 7 Dec 2015; published 21 Dec 2015

which are plotted in Fig. 3 as a function of the index modulation strength Δn for $n_1 = n_3 = 1.0$. At the index modulation strength $\Delta n = 2.2\times10^{-5}$, the transmittance, T_{-1}, of -1 order mode is maximum with the value unity and correspondingly the transmittance, T_0, of 0 order mode is minimum with the value zero. The reflectances are also zero at this critical point. The index modulation strengths of 1.1×10^{-5} and 4.3×10^{-5} are a pair of turning points because the trend in the variation of the transmittances reverses, i.e., $T_{-1} < T_0$ after these two points. The fifth graph, which is designated by CoE, is determined using the conservation of energy as given by the left hand side of Eq. (24). Its value of unity for different values of Δn validates the results of the coupled mode theory for two-dimensional refractive index modulation.

The diffraction efficiency is plotted as a function of the incident angle θ_{in} in Fig. 4 for a fixed acoustic frequency of 75 MHz and different index modulation strengths. It has the maximum value of unity at the Bragg angle of $\theta_{in} = 0.324^o$ at this frequency for the optimal index change of 2.2×10^{-5}. The curves are symmetric about this angle, indicating that the diffraction efficiency reduces by the same amount if the incident light is misaligned to either side of the Bragg angle of incidence. As the index modulation strength deviates more from the optimal Δn, the diffraction efficiency decreases further and varies with θ_{in} more nonuniformly. Good uniformity in the curve shows that the AOD can be operated at nearly 100% diffraction efficiency over a relatively large range of the incident angle and therefore, the AOD would be highly tolerant of misalignment while setting it up and tuning to achieve the Bragg angle of incidence in practice.

Figure 5 examines the diffraction efficiency as a function of the incident angle θ_{in} for different acoustic frequencies and $\Delta n = 2.2\times10^{-5}$. This value of Δn is the optimal index modulation strength at the frequency F = 75 MHz. The Bragg diffraction condition is satisfied only at $\theta_{in} = 0.324^o$ for the frequency of 75 MHz. The diffraction efficiency is nearly 100% and varies symmetrically in the proximity of this angle, but the curve becomes asymmetric away from this angle because Eqs. (8) and (9) hold good around the Bragg angle of incidence. For the other two RF frequencies of 65 MHz and 85 MHz, the Bragg angles are 0.281° and 0.367°, respectively. Although the Bragg condition is satisfied at these two angles, the diffraction efficiency is not unity at the corresponding frequencies because the efficiency of an AOD depends on both the index modulation strength and the degree to which the momentum is conserved in the photon-phonon interaction [29,30]. While the frequency of the acoustic wave affects the conservation of momentum for a given incident light, the acoustic amplitude influences Δn. Therefore, both the frequency F, and the amplitude or equivalently Δn, need to be adjusted to optimize the diffraction efficiency.

#253296 Received 5 Nov 2015; revised 3 Dec 2015; accepted 7 Dec 2015; published 21 Dec 2015

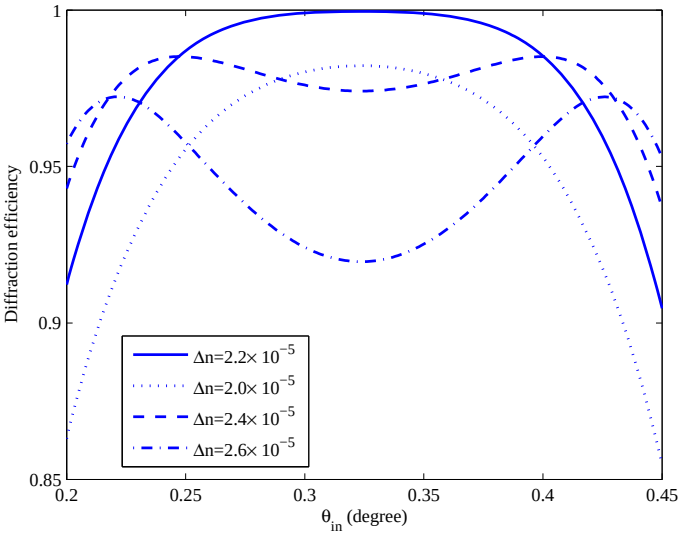

Fig. 4. Diffraction efficiency as a function of the incident angle θ_{in} with L = 2.24 cm, Q = 4π and F = 75 MHz for different index modulation strengths Δn.

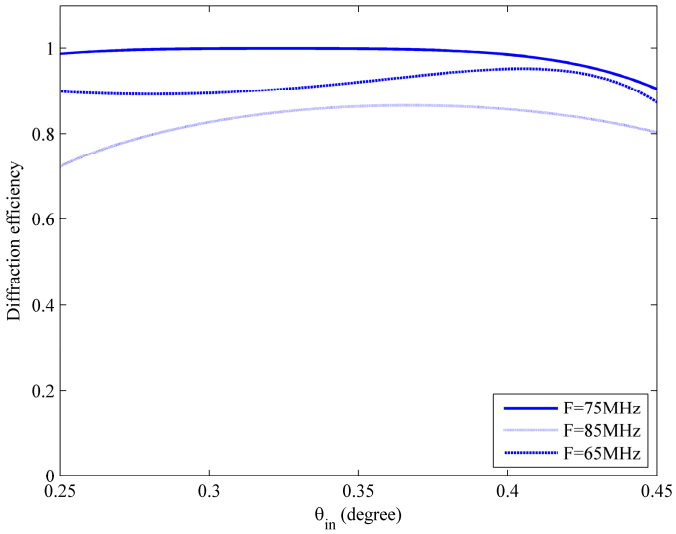

Fig. 5. Diffraction efficiency as a function of the incident angle θ_{in} with $\Delta n = 2.2 \times 10^{-5}$, Q = 4π for different RF frequencies.

#253296 Received 5 Nov 2015; revised 3 Dec 2015; accepted 7 Dec 2015; published 21 Dec 2015

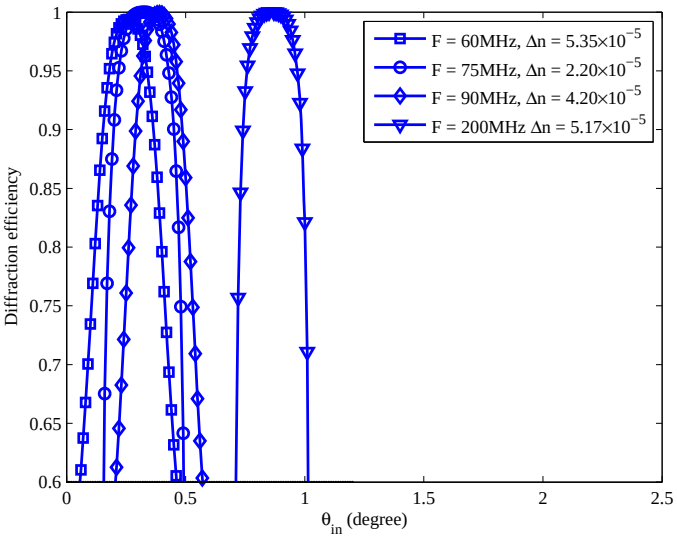

Fig. 6. Diffraction efficiency as a function of the incident angle θ_{in} for $Q = 4\pi$.

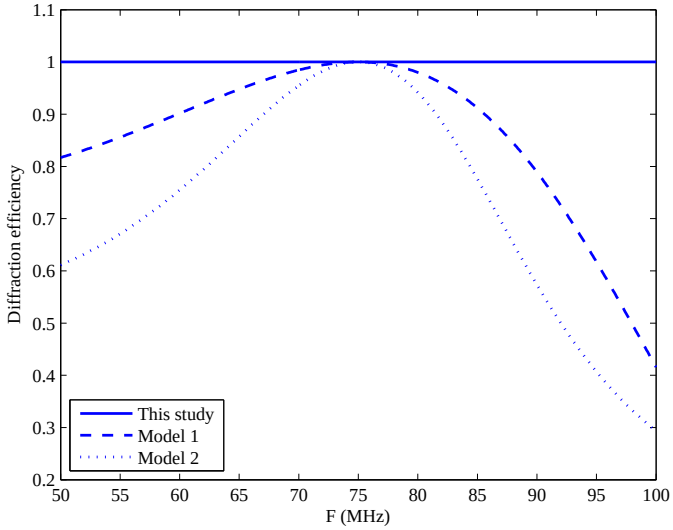

Fig. 7. Comparison of the diffraction efficiency obtained from different models.

The effect of the optimal pair of F and Δn is studied in Fig. 6, which shows the performance of dynamic phase gratings, i.e., acoustic lobes at different steering angles. The diffraction efficiency is plotted as a function of the incident angle θ_{in} for different pairs F and Δn, so that each pair has its own Bragg angle of incidence. This is the reason for achieving 100% diffraction efficiency at different frequencies. As discussed earlier in this section, operating the piezoelectric transducers at different phase-shifts forms acoustic lobes in the AOD at various steering angles, resulting in new incident angles $\theta_0 + \tilde{\theta}$. For each new angle of incidence, an acoustic frequency can be selected to ensure that the Bragg diffraction condition is satisfied. Also the transducers can be operated in the amplitude modulation mode so that the acoustic pressure inside the AOD is sufficient to induce an optimal Δn. Thus the

#253296 Received 5 Nov 2015; revised 3 Dec 2015; accepted 7 Dec 2015; published 21 Dec 2015

phase, frequency and amplitude modulations of the transducers enable achieving 100% diffraction efficiency with relatively large deflection angles at different frequencies.

Figure 7 compares the results of this study with two other models to examine the effect of two-dimensional and one-dimensional refractive index modulations on the diffraction efficiency. This study is based on steerable acoustic lobes, whereas models 1 and 2, which were developed by Kong [14], and Uchida and Niizeki [13], respectively, considered conventional AODs composed of a single or multiple transducers. Models 1 and 2 in Fig. 7 show that conventional AODs have the maximum diffraction efficiency only at the Bragg angle corresponding to the central operating frequency of the AOD, which is 75 MHz in this study, and have limited bandwidth as imposed by the Bragg interaction. Only certain momentum components of the acoustic beam, which can be phase-matched to the momentum components of the incident and diffracted lights, are useful for generating the −1 order mode from the 0 order mode. In the acoustic lobe steering model of this study, however, the diffraction efficiency is 100% for all operating frequencies of the AOD because the Bragg diffraction condition can be achieved at all frequencies as discussed previously.

It should be noted that an ideal, i.e., a loss-less acousto-optic device, is considered in this study. In practice, however, the acousto-optic crystals can absorb the light causing a significant amount of power loss, which will reduce the diffraction efficiency. Additionally, the piezoelectric transducers are not ideal, i.e., they do not generate acoustic waves at a single frequency, which can also affect the diffraction of the light. The diffraction efficiency is 100% in loss-less media as predicted by models 1 and 2, and the model of this study. Klein and Cook's [3] model also yielded 100% diffraction efficiency for isotropic media under certain operating conditions. For anisotropic media, Kastelik et al. [2] determined 100% diffraction efficiency theoretically, which compares well with their experimental data, over a fairly wide range of acoustic frequency under the no power loss condition. These results highlight that all of the light can be diffracted into the first-order mode for ideal AODs.

4. Conclusion

A two-dimensional refractive index model has been presented to modulate the refractive index in two dimensions for improved performance of AODs. The refractive index varies as periodic and sinc functions in the longitudinal and transverse directions, respectively. This type of modulation can be achieved by operating the piezoelectric transducers of AODs in the phase, frequency and amplitude modulation modes simultaneously. The resulting second order coupled mode equations have been solved analytically for the reflection and transmission coefficients of the AOD. The phased array of transducers allows generating tilted acoustic wavefront dynamically, resulting in acoustic lobe steering that produces dynamic two-dimensional phase grating inside the AOD. Due to this effect, the AOD can be operated under the Bragg diffraction condition at any frequency with corresponding optimal index modulation strength and consequently, the diffraction efficiency is found to be unity at different frequencies with relatively large deflection angles. Therefore, the performance of AODs under the two-dimensional index modulation is not limited by the frequency bandwidth as observed in conventional AODs.

Acknowledgments

This work has been supported by the Intel Corporation under the contract No. UCF-CONV001712.

#253296 Received 5 Nov 2015; revised 3 Dec 2015; accepted 7 Dec 2015; published 21 Dec 2015